STABILITY MARGIN ANALYSIS IN MULTIOBJECTIVE DESIGN: APPLICATION TO AN AEROSPACE LAUNCHER

Mohamed ABBAS-TURKI [*], **Gilles DUC** [*]
Benoît CLEMENT [**]

[*] *École Supérieure d'Electricité, Service Automatique, 3 rue Joliot Curie, 91192 Gif-sur-Yvette cedex, France*
mohamed.abbas-turki@supelec.fr and gilles.duc@supelec.fr
[**] *CNES, Direction des Lanceurs, Rond Point de l'Espace, 91023 Every cedex, France*
benoit.clement@cnes.fr

Abstract: To check the stability margins the designers commonly use the graphical method which is very constraining when the verification must be done several times, as for instance when a routine is to be developped. In this paper a practical method is proposed, based on the Kalman-Yakubovich-Popov (KYP) lemma. This method avoids the conservatism induced by $\mathcal{H}_\infty$ analysis and a huge calculation as the one derived by μ-analysis.

Keywords: Gain margin, Phase margin, Delay margin, KYP lemma.

1. INTRODUCTION

The stability margins are the mostly used constraints specified by the manufacturer to translate the robust stability. To determine them without using the classical graphical method, a $\mathcal{H}_\infty$ analysis can be done by using the small gain theorem, but it is known to be conservative since the gain and phase (or delay) variations are mixed in the same uncertainty. A better way is to use μ-analysis but it leads to an important number of added variables, despite of its accuracy.

The problem considered in this paper is to determine with a good accuracy the value of the margins without involving a huge calculation. Although the Matlab function *allmargin* gives a good accuracy in most cases, the results can be inadequate because they are based on computing the frequency response for a finite number of frequencies and a linear interpolation between the obtained values is used. In this paper a method is developed to avoid such an interpolation.

Furthermore, the aim is not only to present a method for analysis, which each department of automatic control has already developed, but to find a method which can be further expanded to a multiobjective controller synthesis, as it is the case for $\mathcal{H}_\infty$ and μ analyses.

This paper is influenced by the works of Kao (Kao, 2002; Kao and Jönsson, 2000), where the Kalman-Yakubovich-Popov (KYP) lemma is used to overcome the added variables introduced in a classical Linear Matrix Inequality (LMI) problem. In this paper the eigenvalues of a Hamiltonian matrix are taken into consideration to check a passivity constraint, without having to solve an LMI problem (which can be harsh for plants with badly damped modes).

For the phase and delay margins, a bilinear approximation is used to formalize the problem into

the Linear Fractional Transfer (LFT) form. Such an approximation is not necessary for the gain margin.

Only the case of SIMO plants (one control input with possibly several measurements) is considered in this paper, which is the major case in aerospace plants like a launcher or a satellite (when each axis can be considered separately). This work can be extended to MIMO plants by considering the same margin for all inputs.

The paper is organized as follows: section 2 explains the transformations used to lead the problem to the LFT form for the gain, phase and delay margins successively; the main results appear in section 3, where the constraints enable to determine the values of the margins. An application on an aerospace launcher is finally presented in section 4.

2. LFT FORMS FOR MARGIN ANALYSIS

The common way to perform robust stability analyses is to put an uncertain plant in the LFT form, which allows the use of the small gain theorem. This form is also used in this paper, but the passivity is used instead of the small gain theorem.

Consider a continuous or discrete-time plant G with state space realization:

$$G: \begin{array}{c} \\ \rho x \\ z \\ y \end{array} \begin{array}{c} \begin{array}{ccc} x & w & u \end{array} \\ \left(\begin{array}{c|cc} A & B_1 & B_2 \\ \hline C_1 & D_{11} & D_{12} \\ C_2 & D_{21} & D_{22} \end{array}\right) \end{array} \tag{1}$$

where z is the output to be controlled despite disturbance w, using control input u and measurement y; ρ represents either the derivative or the advance operator. In the case of stability margins for SIMO plants, the transfer between w and z is scalar and represented by an uncertainty δ, whose maximal allowable variation is the image of the margin variation.

Considering a stabilizing controller K, the closed-loop plant is given by the Redheffer product $G_{zw} = G * K$ (see the interconnection structure of Figure 1), which enables the stability analysis with respect to δ.

Remark. Note the input w is multiplied by -1, to allow the use of the Nyquist theorem in the stability analysis.

2.1 Gain margin

Two types of gain margins can be considered: the first one is the Reduction Gain Margin (RGM),

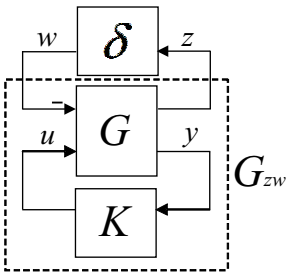

Fig. 1. Closed-loop structure for stability margin analysis

which guarantees the stability for gains less then one. The second is the Increasing Gain Margin (IGM), which concerns gains higher than one. As is commonly known, the gain margin can be simply put in the LFT form of Figure 2:

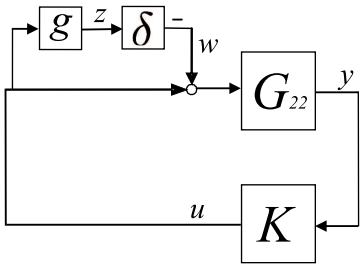

Fig. 2. Closed-loop structure for gain margin analysis

with $G_{22} = \left(\begin{array}{c|c} A & B_2 \\ \hline C_2 & D_{22} \end{array}\right)$, δ varying in $[0, 1]$ and $g = 1 - 10^{\frac{GM}{20}}$, where GM equals either the RGM or IGM with dB unit. The corresponding state space representation of G is then:

$$G: \begin{array}{c} \\ \rho x \\ z \\ y \end{array} \begin{array}{c} \begin{array}{ccc} x & w & u \end{array} \\ \left(\begin{array}{c|cc} A & B_2 & B_2 \\ \hline (0 \ldots 0) & 0 & g \\ C_2 & D_{22} & D_{22} \end{array}\right) \end{array} \tag{2}$$

2.2 Phase margin

The phase margin is given by multiplying plant G_{22} by $e^{i\theta}$ (Figure 3), where θ is the phase margin.

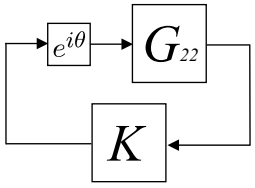

Fig. 3. Phase margin representation

The idea for getting the LFT form of Figure 1 is to replace $e^{i\theta}$ by a rational function also describing the unit circle:

$$e^{i\theta} = \frac{1 + i\hat{\theta}}{1 - i\hat{\theta}} \tag{3}$$

Note that for $\theta \in [0, \theta_e]$, $\hat{\theta}$ is real and belongs to $\left[0, \frac{e^{i\theta_e}-1}{i(e^{i\theta_e}+1)}\right]$.

Equation (3) can be realized as the interconnection $i\hat{\theta} * \mathcal{N}$, with:

$$\mathcal{N} = \begin{pmatrix} 1 & 1 \\ 2 & 1 \end{pmatrix} \tag{4}$$

The problem can then be formulated in LFT form, with $\delta \in [0, 1]$, as shown in Figure 4.

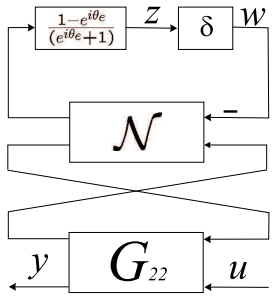

Fig. 4. Closed-loop structure for phase margin analysis

The corresponding state space representation of G is then:

$$\begin{array}{c} \\ \rho x \\ z \\ y \end{array} \begin{array}{c} \begin{array}{ccc} x & w & u \end{array} \\ \left(\begin{array}{c|cc} A & 2B_2 & B_2 \\ \hline (0\ldots0) & \hat{g} & \hat{g} \\ C_2 & 2D_{22} & D_{22} \end{array}\right) \end{array} \tag{5}$$

where $\hat{g} = \dfrac{1 - e^{-i\theta_e}}{1 + e^{-i\theta_e}}$

2.3 Delay margin

The delay margin is derived from the phase margin θ as:

$$\tau = \frac{\theta}{\omega_0} \tag{6}$$

where ω_0 is the maximal frequency ω, such that $|G_{zw}(i\omega)| = 1$.

For finding ω_0, the KYP lemma will be used once again, as explained in the next section along with a method for the analysis of the closed loop plant with uncertainty $\delta \in [0, 1]$.

3. DETERMINATION OF THE STABILITY MARGINS

The computation of the stability margins will be based on the state-space representations (2) (for the gain margins) and (5) (for the phase margin). These realizations are obtained for given fixed values of g and θ_e respectively: they will allow to test if the corresponding margin is at least equal to this value. To obtain the best evaluation of the margin, the test will be repeated by applying a bisection algorithm on a given interval, just like for the classical computation of the $\mathcal{H}_\infty$ norm.

Only the continuous case will be considered: for discrete-time plants, the analysis can be done by applying first a Tustin transformation.

Note first that according to the Nyquist theorem, the closed-loop plant of Figure 2 or 4 remains stable for all $\delta \in [0, 1]$ iff the Nyquist plot of G_{zw} doesn't intersect the real axis on interval $(-\infty, -1]$. A first sufficient condition is that the real part of $G_{zw}(i\omega)$ always remains greater than -1, which can be written:

$$H(i\omega) = (G_{zw}(i\omega) + 1) + (G_{zw}(i\omega) + 1)^* > 0 \quad \forall \omega \in [0, \infty) \tag{7}$$

This is a passivity constraint which can be checked using the KYP lemma by the approach proposed below. Although it is generally efficient for rigid models, it can be too conservative, especially for plants with bending modes. The proposed approach is therefore more general.

The key idea is to look for the points where the Nyquist plot of G_{zw} intersects the real axis, and (if there exist) to check if they are on the right of -1. Equivalently, by applying a $+\frac{\pi}{2}$ rotation to the Nyquist plot, one has to look for the intersections with the imaginary axis. Such a rotation is simply obtained by replacing the C and D matrices of G_{zw} by iC and iD respectively.

The KYP lemma can now be used to test if the Nyquist plot remains on the right-half plane (which is a passivity constraint) and, if not, to determine the intersection points. Although it gives several equivalent conditions (see for instance (Iwasaki and Hara, 2003)), only two of them will be considered.

Lemma 1. Let the matrix function:

$$H(i\omega) = \begin{pmatrix} \hat{G}(j\omega) \\ I \end{pmatrix}^* \begin{pmatrix} Q & F \\ F^* & R \end{pmatrix} \begin{pmatrix} \hat{G}(j\omega) \\ I \end{pmatrix} \tag{8}$$

where $\hat{G}(i\omega) = (i\omega I - A)^{-1} B$, $Q = Q^*$, $R = R^*$, and A is Hurwitz. Assume the pair $[A, B]$ is stabilizable. The following statements are equivalent:

(1) $H(i\omega) > 0$, $\forall \omega \in [0, \infty)$.
(2) $R > 0$, and the Hamiltonian matrix $\mathcal{H}$ has no eigenvalues on the imaginary axis

where $\mathcal{H}$ is defined by:

$$\mathcal{H} = \begin{pmatrix} A - BR^{-1}F^* & BR^{-1}B^* \\ Q - FR^{-1}F^* & -A^T + FR^{-1}B^* \end{pmatrix} \tag{9}$$

The passivity constraint is obtained for :

$$\begin{aligned} Q &= \mathbf{0} \\ F &= C^* \\ R &= D^* + D \end{aligned}$$

If after the rotation one obtains $real(D) = 0$ then R will be replaced by $R = D^* + D + \varepsilon$, where $\varepsilon > 0$ is a small real number. This means that the KYP lemma checks if the Nyquist plot always remains with a real part greater than $-\varepsilon$ or equivalently if the original Nyquist plot always has an imaginary part greater than $+\varepsilon$. To avoid the case where there is an intersection between the axis $y = i\varepsilon$ but there is none with the real axis (Figure 5), a second condition is added, which is $H(i\omega) < 0$ with $R = D^* + D - \varepsilon$, where ω must have the same sign in both intersections.

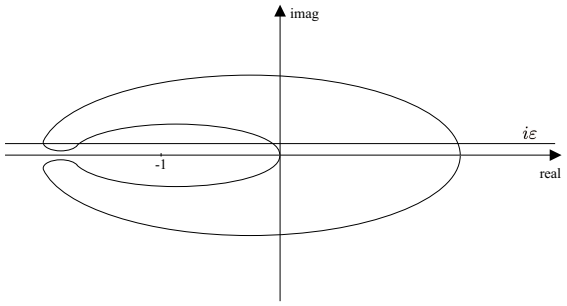

Fig. 5. Example of the usefulness of two passivity constraints

In the case where $real(D) < 0$ the condition (1) of Lemma 1 is replaced by $H(i\omega) < 0$.

The important point is that the values of ω for which the original Nyquist plot intersects the real axis correspond exactly to the imaginary eigenvalues of the Hamiltonian matrix if the passivity constraint is not verified.

Proof. The equivalence induced in lemma 1 is mainly due to the fact that if $\hat{\omega}$ is a solution of $H(i\hat{\omega}) = 0$, then $i\hat{\omega}$ is the eigenvalue of the Hamiltonian matrix $\mathcal{H}$.

To establish this fact, a state space representation of H can be derived by writing H successively as:

$$\begin{aligned} H : & \left(\left(\begin{array}{c|c} A & B \\ \hline I & 0 \end{array}\right) \right)^* \begin{pmatrix} Q & F \\ F^* & R \end{pmatrix} \left(\left(\begin{array}{c|c} A & B \\ \hline I & 0 \end{array}\right) \right) \\ & \qquad I \\ H : & \left(\begin{array}{c|c} A & B \\ \hline I & 0 \\ \hline 0 & I \end{array}\right)^* \begin{pmatrix} Q & F \\ F^* & R \end{pmatrix} \left(\begin{array}{c|c} A & B \\ \hline I & 0 \\ \hline 0 & I \end{array}\right) \\ H : & \left(\begin{array}{cc|c} -A^T & Q & F \\ \hline -B^* & F^* & R \end{array}\right) \left(\begin{array}{c|c} A & B \\ \hline I & 0 \\ \hline 0 & I \end{array}\right) \\ H : & \left(\begin{array}{cc|c} A & 0 & B \\ Q & -A^T & F \\ \hline F^* & -B^* & R \end{array}\right) \end{aligned}$$

The zeros of the transfer function H are the poles of H^{-1} for $R \neq 0$, which are the eigenvalues of:

$$\begin{pmatrix} A & 0 \\ Q & -A^T \end{pmatrix} - \begin{pmatrix} B \\ F \end{pmatrix} R^{-1} \begin{pmatrix} F^* & -B^* \end{pmatrix} = \begin{pmatrix} A - BR^{-1}F^* & BR^{-1}B^* \\ Q - FR^{-1}F^* & -A^T + FR^{-1}B^* \end{pmatrix}$$

which is exactly $\mathcal{H}$.

Finally, for checking if the chosen value of the stability margin is satisfied, the values of $\hat{\omega}$ are replaced on G_{zw} and if the real parts are all greater than -1, then this value of the margin is verified (the imaginary part should be equal to zero or negligible).

Since for the gain margin D is complex (after the $+\frac{\pi}{2}$ rotation), the use of ε is required. For the phase margin, D is a real scalar.

According to these developments, the delay margin can also be calculated by using the value of the phase margin and looking for ω_0 in (6). The constraint to be checked is:

$$\hat{H}(i\omega) = 1 - G_{zw}(i\omega)G_{zw}^*(i\omega) > 0 \; \forall \omega \in [0, \infty) \quad (10)$$

which is obtained by the following new values of Q, F and R:

$$\begin{aligned} Q &= C^T C \\ F &= -C^T D \\ R &= -D^T D + 1 \end{aligned}$$

Using the corresponding Hamiltonian matrix, the maximum absolute value of all eigenvalues located on the imaginary axis is ω_0. An example of application will be given in the following section to show the efficiency of the approach.

4. APPLICATION TO AN AEROSPACE LAUNCHER

The application is developed for the yaw axis of an European space launcher (figure 6), whose dynamics include three rigid modes and five bending modes (the sloshing modes are not considered). The main launcher disturbance is the wind speed W, which does not occur directly on the input command β (the angle of nozzle deflection), nor on the measured output ψ (the attitude angle). The rigid state space model can be written as:

$$\begin{cases} \dfrac{d}{dt} \begin{pmatrix} \psi \\ \dot{\psi} \\ \dot{z} \end{pmatrix} = A \begin{pmatrix} \psi \\ \dot{\psi} \\ \dot{z} \end{pmatrix} + \begin{pmatrix} B & B_W \end{pmatrix} \begin{pmatrix} \beta \\ W \end{pmatrix} \\ y = \begin{pmatrix} 1 & 0 & 0 \end{pmatrix} \begin{pmatrix} \psi \\ \dot{\psi} \\ \dot{z} \end{pmatrix} \end{cases} \quad (11)$$

This model is increased by a 2nd order model of the actuator, while the sensor is considered as a constant gain.

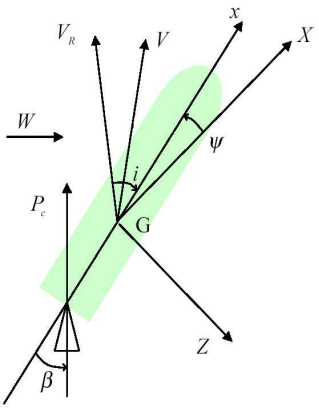

Fig. 6. Two dimensions launcher representation

Several multiobjective compensators have been proposed to this problem: see (Clement, 2001; Voinot, 2002; Abbas-Turki *et al.*, 2004) and the references given in (Imbert and Clement, 2004). In this study, the stability margins of the compensator given in (Abbas-Turki *et al.*, 2004) are analyzed.

Among all the manufacturer specifications (Clement *et al.*, 2001), the following stability margins have been specified:

- decreasing and increasing gain margins at least equal to ΔG_{LF} and ΔG_{HF} respectively
- time delay at least equal to the sample-time T_e.

The Nichols plot for the open loop plant with the compensator is showed in Figure 7. The values of the gain, phase and delay margins given by the Matlab function *allmargin* are:

- decreasing gain margin: $2.36 \times \Delta G_{LF}$
- increasing gain margin: $2.14 \times \Delta G_{HF}$
- delay margin: $1.43 \times T_e$

whereas the proposed approach gives the following values:

- decreasing gain margin: $2.35 \times \Delta G_{LF}$
- increasing gain margin: $2.14 \times \Delta G_{HF}$
- delay margin: $1.86 \times T_e$

Although the difference seems to be insignificant, one has to take into account that even a small difference can have a significant effect if such an analysis is included in a synthesis procedure. Note finally that the value given by the proposed method has been verified by including a Padé approximation of the delay in the feedback loop and computing the closed-loop eigenvalues.

5. CONCLUSION

This paper gives improvements on analyzing the stability margins. The numerical efficiency of the proposed technique has been showed by considering the analysis of an aerospace launcher. The

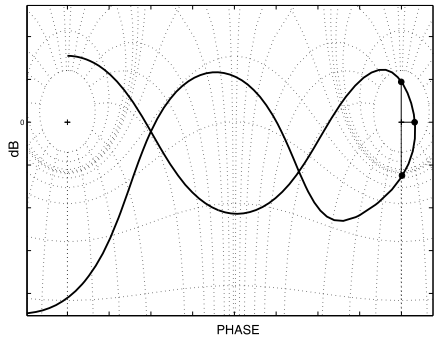

Fig. 7. Nichols chart of the controlled plant

interesting point is that no interpolation method is used, which is very promising for expanding this method into a synthesis one.

Indeed the passivity constraint is a convex one, which allows the use of various algorithms such as the Cutting Plane Algorithm of (Kao, 2002; Kao and Jönsson, 2000). Note however that due to the restrictions to a certain interval of intersection, the problem becomes nonconvex, so that the convergence of these algorithms is no longer guaranteed. It is therefore a subject for future research.

6. ACKNOWLEDGEMENT

The authors thank the Launch Division of the French Space Agency (CNES/DLA) for supporting this work.

REFERENCES

Abbas-Turki, M., G. Duc and Benoit Clement (2004). Robust control of a space launcher by introducing lqg/ltr ideas in the ncf robust stabilisation problem. *16th IFAC Symposium on Automatic Control in Aerospace.*

Clement, B. (2001). Synthèse multiobjectifs et séquencement de gains: Apllication au pilotage d'un lanceur spatial. PhD thesis. Université Paris XI Orsay.

Clement, B., G. Duc, S. Mauffrey and A. Biard (2001). Gain scheduling for an aerospace launcher with bending modes. *15th IFAC Symposium on Automatic Control in Aerospace* pp. 475–480.

Imbert, N. and B. Clement (2004). Launcher attitude control: some answers to the robustness issue. *16th IFAC Symposium on Automatic Control in Aerospace.*

Iwasaki, T. and S. Hara (2003). Generalized kyp lemma: Unified characterization of frequency domain inequalities with applications to system design. *Mathematical Engineering Technical Reports.*

Kao, C.-Y. (2002). Efficient Computational Methods for Robustness Analysis. PhD thesis. Massachusetts Institute of Technology.

Kao, C.-Y. and U. T. Jönsson (2000). An algorithm for solving optimization problems involving special frequency dependent lmis. *American Contr. Conf.* pp. 307–311.

Voinot, O. (2002). Développement de méthodologies de synthèses de lois de commande pour le pilotage des lanceurs. PhD thesis. Ecole Nationale de l'Aéronautique et de l'Espace.